International Journal of Electrical, Energy and Power System Engineering
Vol. 09, No. 03, October 2026
e-ISSN: 2654-4644

Optimizing Load Aggregator Operations Integrating Distributed Energy and Demand Response

Nhung Nguyen-Hong[1*], Khang Trieu-Phuc[2], Quan Tran-Duc[3]
[1,2,3] School of Electrical and Electronic Engineering, Hanoi University of Science and Technology, Vietnam
[1]nhung.nguyenhong1@hust.edu.vn, [2] Khang.TP212369@sis.hust.edu.vn,
[3]Quan.TD212385@sis.hust.edu.vn

[*]Corresponding author, nhung.nguyenhong1@hust.edu.vn

Abstract— The increasing penetration of customer side photovoltaic (PV) generation, energy storage systems (ESSs), and flexible demand requires coordinated scheduling by load aggregators (LAs). This study develops a mixed integer linear programming model for day ahead LA operation under Vietnam's time of use tariff. The model coordinates grid purchases, PV generation, ESS charging and discharging, and four demand categories: rigid, curtailable, transferable, and shiftable loads. Its main contribution is a shiftable load formulation that preserves rated operating power and uninterrupted operating duration after rescheduling. The model is implemented in GAMS and solved using CPLEX for three operating scenarios. Under the stated short term operating cost assumptions, daily net operating profit increases from 0.276 million VND in the grid only scenario to 21.518 million VND with PV and ESS and to 29.360 million VND when demand response is also enabled. At hour 12, grid purchases in the PV ESS DR scenario are approximately 32% of those in the grid only scenario. The results indicate the operational value of coordinated scheduling; however, they do not constitute a complete investment feasibility assessment.

Keywords: Demand response, Flexible load, Load aggregator, Optimal scheduling, Renewable energy.

This work is licensed under a CC BY-NC. Copyright ©2026 by Author. Published by Universitas Riau.

INTRODUCTION

The share of renewable energy sources (RESs), especially wind and photovoltaic (PV) generation, has been increasing in modern power systems. This trend helps reduce fossil fuel consumption and supports carbon-neutrality targets, but it also brings operational challenges due to the variability of RES output. At the same time, electricity demand continues to grow, particularly in developing countries. In Vietnam, electricity consumption has been growing by more than 10% annually due to economic expansion, industrialization, and urbanization [1]. Together with the rapid deployment of customer-side PV, this demand growth can widen the peak to valley difference in the load curve, making peak regulation and system balancing more difficult. Relying solely on traditional regulatory resources, such as

Received: June 5, 2026, Revised: Sept 3, 2026, Accepted: Sept 20, 2026
https://doi.org/10.31258/ijeepse.9.3.149-164

standby or peaking generation units, may entail high investment costs while offering limited utilization efficiency.

To address these issues, Load Aggregator (LA) models have attracted increasing attention [2-4]. An LA manages a group of customers as a single operational entity, purchasing electricity from the grid and reselling it to end users [5-7]. This structure is well suited for demand response (DR), as the LA can coordinate dispersed flexible loads more effectively than direct individual control [2, 8]. Through incentive-based or direct-control mechanisms, DR can reduce peak demand, improve renewable energy utilization, and support more efficient system operation.

In the literature, many studies have focused on optimizing the operation of LAs and coordinating their internal DR resources to maximize profit. Recent work has considered LA decision-making in energy and reserve markets [9], flexible load aggregation for distribution system operation [10], and robust scheduling of generation load aggregators under renewable and demand uncertainty [11]. Other studies have investigated joint bidding and incentive strategies for price-maker LAs [12] and demand response participation of heterogeneous flexible load aggregators [13], and distribution system scheduling with LA participation to reduce operating costs, network losses, and renewable energy curtailment [14]. These works confirm the growing role of LAs in demand-side flexibility and power system operation.

More closely related to DR load modelling, the study [3] considers an industrial park including electric vehicles (EVs), reducible loads, and shiftable loads, and proposes an optimal scheduling and compensation-pricing method for LAs to meet peak-shaving needs under a limited budget, aiming to reduce associated scheduling costs. Similarly, a combined dispatching model for Load Aggregators managing four types of customer side flexible loads: industrial users, central air conditioning, electric vehicles, and energy storage stations, is developed in [4] to minimize operating costs. The combined scheduling leverages the complementary advantages of various load characteristics to effectively achieve peak shaving, valley filling, and promote renewable energy integration. In [6], the authors propose a demand-side resource aggregation optimization model for indirect users that utilizes load reduction and load transfer contracts to maximize LA revenue and stabilize spot market prices. This study also reduces the System Power Shortage Index and narrows the peak-valley difference in power consumption. In [15], a tiered compensation pricing strategy for Load Aggregators managing controllable loads, including storage and distributed generation, is proposed to mitigate the financial penalties resulting from deviations between bid volumes and actual consumption in the electricity market. In [16], the authors consider residential consumers whose loads are decomposed into five types (shiftable, controllable, storable like EVs, on demand, and base loads). The LA's profit is maximized by determining the optimal hourly bid quantity in day ahead markets while minimizing penalty costs resulting from deviations between expected and actual load values under Demand Response (DR) uncertainty. A multi-agent collaborative operation framework is developed in [17] to coordinate hydrogen based steel plants, which exhibit both rigid and flexible load components, with Internet Data Centers (IDCs) and EV aggregators. The main objective is to minimize the total operating cost while ensuring the completion of production tasks under extreme scenarios where a limited power supply constrains industrial operations. Overall, these studies provide useful foundations for LA scheduling, but they also indicate that the detailed modelling of different flexible load types remains an important issue.

However, in the above studies, the discussion of DR load types is not fully comprehensive. Most works such as [4], [6], and [15] focus mainly on curtailable and transferable loads, with limited attention to shiftable loads. Shiftable loads are considered in [3], but they are mainly represented through energy balance and minimum operating time constraints. More recent

work has also discussed uninterruptible time-shiftable loads [18], showing that operating continuity is an important practical requirement. However, in LA scheduling models that coordinate PV, ESS, and multiple DR load types, there is still a need for a shiftable load formulation that preserves both rated operating power and the full continuous operating duration at the individual customer level. Without this level of modelling detail, the optimized schedule may not be fully suitable for practical devices such as production machinery, pumping systems, or large HVAC units.

This paper develops a mixed integer linear programming (MILP) based operational optimization model for an LA that manages four load types: rigid, curtailable, transferable, and shiftable. The main novelty of the proposed load modelling approach lies in the shiftable-load formulation. Unlike simplified shiftable load formulations, the proposed model treats each shiftable load as a complete operating block and preserves both its rated operating power and continuous operating duration after rescheduling. This makes the scheduling result more suitable for practical customer-side equipment whose operation cannot be interrupted or partially reshaped. The LA also integrates PV and ESS resources to reduce grid dependence and store energy during low-price periods. Under a TOU electricity purchase tariff and a fixed selling price to customers, the LA coordinates grid purchasing, PV generation, ESS operation, and DR actions to maximize its net profit. The proposed model is tested using Vietnam's electricity tariff and solved in GAMS [19] and CPLEX [20].

The rest of this paper is organized as follows. Section 2 presents the method and mathematical formulation of the proposed LA model. Section 3 discusses the case study and simulation results. Section 4 concludes the paper.

METHOD

This study optimizes the operational strategy of an LA integrating PV, ESS, and DR, as illustrated in Figure 1. The LA acts as an intermediary that purchases electricity from the main grid under a TOU tariff and resells it to end users. From the grid's perspective, the LA is treated as a large consumer whose demand can be managed through internal resources and flexible loads.

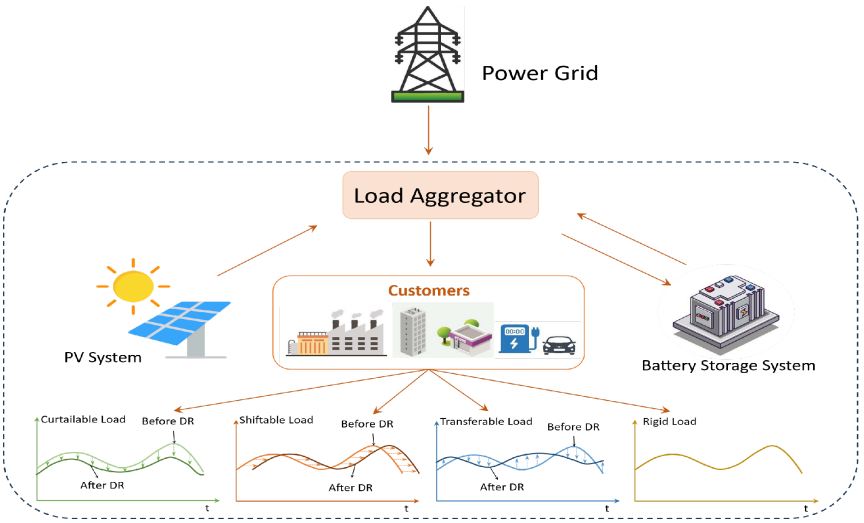


Figure 1. The LA model's description

To reduce electricity procurement costs and improve operational efficiency, the LA coordinates the available PV output, ESS charging/discharging operation, and DR actions. Customer loads are classified into four types according to their flexibility. Rigid loads must be supplied as scheduled and cannot be adjusted. Curtailable loads can be reduced within

predefined limits during DR events. Shiftable loads can be moved as a whole to other time periods while maintaining their required continuous operating duration. Transferable loads allow part of their energy consumption to be redistributed across time periods with greater scheduling flexibility.

Transferable, shiftable, and curtailable loads can be encouraged to adjust their consumption patterns and then receive incentive payments. Under the TOU tariff, the LA coordinates these flexible loads together with other components. In practice, the ESS charges during low-price periods and discharges during peak hours, while demand response shifts or reduces consumption when prices are high. As a result, the LA can effectively reduce grid power purchases during peak hours, enhance energy self-consumption, and contribute to a more balanced and sustainable power system. The optimization model developed in this section determines the electricity purchase and sales plan, the ESS operation schedule, and the regulation of different load types to maximize the LA's overall profit.

The proposed MILP model is applied to a one-day scheduling horizon divided into 24 hourly intervals. The required inputs include customer load profiles, available PV output, TOU electricity tariffs, DR incentive rates, and PV–ESS operating parameters. The load profiles are synthetically generated and calibrated to represent typical demand characteristics in Vietnam. It is assumed that the day-ahead load demand and PV availability are forecasted in advance, and that the LA purchases electricity from the grid without selling electricity back. The detailed numerical data are presented in the Case Study subsection of the Results and Discussion section.

A. Objective Function

The objective function is designed to maximize the LA's net operating profit by balancing electricity sales revenue against the major operating costs. These costs include grid electricity procurement cost, incentive payments for DR participation, PV operating cost, and ESS charging and discharging costs. The complete objective function is given in (1):

$$Maximize\ Z = R_{sell} - C_{buy} - C_{DR} - C_{IR} \quad (1)$$

where the first term R_{sell} represents the electricity sales revenue obtained from the LA's customers and is calculated using (2). In this equation, $pr_{sell}(t)$ denotes the electricity price at which the LA sells power to customers. The terms $P_{rigid}(t)$, $P_{transfer-final}(t)$, $P_{shift-final}(c,t)$, and $P_{curtail-final}(t)$ represent the rigid load demand and the final transferable, shiftable, and curtailable load demands after applying DR at time t, respectively. Besides, Δt is the time interval, set to 1 hour in this study, and CT is the set of shiftable customers, $CT = CT1, \ldots, CTn$.

$$R_{sell} = \sum_{t\in T} C_{sell}(t)\left[\sum_{c\in CT} P_{shift-final}(c,t) + P_{rigid}(t) + P_{transfer-final}(t) + P_{curtail-final}(t)\right]\Delta t \quad (2)$$

The second term C_{buy} represents the total cost of electricity purchased from the grid and is calculated in (3), where $pr_t(t)$ is the grid electricity tariff and $P_{Grid}(t)$ is the power purchased by the LA from the grid at time t.

$$C_{buy} = \sum_{t\in T} pr_t(t) \cdot P_{Grid}(t)\cdot\Delta t \quad (3)$$

The third term C_{DR} represents the total incentive cost paid by the LA to customers

participating in the DR program and is calculated in (4). The first component accounts for curtailable-load compensation, where $P_{c-initial}(t)$, $\alpha(t)$, and $pr_{CD}(t)$ denote the initial curtailable load, curtailment ratio, and curtailable load incentive rate at time t, respectively. The second component represents the incentive paid for shiftable loads, where $pr_{shift}(t)$ is the shiftable load incentive rate, $u_{so}(c,t,i)$ is a binary variable equal to 1 if the shiftable load of customer c is moved from its original operating time t to a new operating time i, and $P_{s-allow}(c)$ is the rated power of customer c's shiftable load. The last component captures the compensation for transferable-load adjustments, where $pr_{DR-up}(t)$ and $pr_{DR-down}(t)$ are the upward and downward transferable load incentive rates, and $P_{DR-up}(t)$ and $P_{DR-down}(t)$ are the corresponding upward and downward adjustments at time t.

$$C_{DR} = \sum_{t\in T}\left[P_{c-initial}(t)\alpha(t)pr_{CD}(t)\right]\Delta t + \sum_{t\in T} pr_{shift}(t) \sum_{c\in CT}\sum_{i\in T} u_{so}(c,t,i)P_{s-allow} \quad (4)$$

The last term C_{IR} represents the operating cost of the LA's internal PV and ESS units and is calculated in (5). Here, $P_{PV}(t)$ and $pr_{PV}(t)$ denote the actual PV output and PV operating cost, while $P_{ESS-charge}(t)$, $P_{ESS-discharge}(t)$, and $pr_{ESS}(t)$ represent the ESS charging power, discharging power, and operating cost, respectively:

$$C_{IR} = \sum_{t\in T}\left[pr_{PV}(t)P_{PV}(t)\Delta t\right] + \sum_{t\in T}\left[pr_{ESS}(t)\left(P_{ESS-discharge}(t) + P_{ESS-charge}(t)\right)\Delta t\right] \quad (5)$$

B. Constraints

The power balance of the LA is expressed in (6), accounting for grid purchases, PV generation, ESS operation, and customer demand after DR adjustments. The total power supplied by the grid, PV, and ESS discharging must equal the adjusted customer demand and ESS charging power at each time interval. Constraint (7) restricts grid power purchases to non-negative values, ensuring that electricity flows only from the grid to the LA.

$$P_{Grid}(t) + P_{PV}(t) + P_{ESS-discharge}(t) = P_{ESS-charge}(t) + \sum_{c\in CT} P_{shift-final}(c,t) + P_{rigid}(t) + P_{transfer-final}(t) + P_{curtail-final}(t), \quad \forall t \in T \quad (6)$$

$$P_{Grid}(t) \geq 0, \ \forall t\in T. \quad (7)$$

The curtailable load constraints define the allowable reduction in customer demand. Equation (8) determines the remaining load after applying the curtailment ratio $\alpha(t)$. Constraint (9) bounds this ratio between zero and $\alpha_{max}(t)$, ensuring that load reduction remains within the prescribed limit.

$$P_{curtail-final}(t) = P_{c-initial}(t)(1 - \alpha(t)), \ \forall t\in T. \quad (8)$$

$$0\leq\alpha(t) \leq \alpha_{max}(t), \ \forall t\in T. \quad (9)$$

For shiftable loads, (10) determines the final demand $P_{shift-final}(c,t)$ of each customer c over the scheduling horizon $T = 1, ..., 24$, where $CT = CT_1, ..., CT_n$ is the set of shiftable customers. The equation starts from the initial load $s_{actual}(c,t)$, subtracts the load shifted out of interval t, and adds the load shifted into that interval. The binary variable $u_{so}(c,t,i)$ equals 1 when the load of customer c is shifted from interval t to interval i. Conversely, $u_{si}(c,t,i)$ represents the incoming load at interval t from interval i.

$$P_{shift-final}(c,\ t) = s_{actual}(c,\ t) + P_{s-allow}(c) \sum_{i\in T\ i\neq t} \left[u_{si}(c,\ t,\ i) - u_{so}(c,\ t,\ i)\right]$$

$$\forall c\in CT,\ \forall t\in T \tag{10}$$

Constraint (11) ensures consistency between the outgoing and incoming shifting decisions. When a load is shifted from interval t to interval i, the corresponding variables $u_{so}(c,t,i)$ and $u_{si}(c,i,t)$ must have the same value. Constraint (12) prevents simultaneous outgoing and incoming shifting within the same interval for a given customer, while (13) excludes shifting a load from an interval to itself.

$$u_{so}(c,\ t,\ i) = u_{si}(c,\ i,\ t),\ \ \forall c\in CT,\ \forall t,\ i\in T. \tag{11}$$

$$\sum_{i\in T\ i\neq t} u_{so}(c,t,\ i) + \sum_{i\in T\ i\neq t} u_{si}(c,t,\ i)\leq 1,\ \ \forall c\in CT,\ \forall t\in T. \tag{12}$$

$$u_{so}(c,t,t) = u_{si}(c,t,t) = 0,\ \forall c\in CT,\ \forall t\in T. \tag{13}$$

Constraint (14) specifies the allowable shifting window for each customer. The shifting variable $u_{so}(c,t,i)$ is set to zero when $i < T_{min}(c)$ or $i > T_{max}(c) - T_{opt}(c) + 1$. Here, $T_{min}(c)$ and $T_{max}(c)$ define the window boundaries, while $T_{opt}(c)$ denotes the required continuous operating duration. The upper limit is intended to ensure that the operating block can be completed within the allowable window.

$$u_{so}(c,t,i) = 0, \forall c\in CT,\ \forall t, i\in T: i < T_{min}(c) \text{ or } i > T_{max}(c) - T_{opt}(c) + 1 \tag{14}$$

Constraint (15) links the shifting decision at the original start time $T_{start}(c)$ to the outgoing decisions over the entire original operating period. This condition is intended to move the complete operating block rather than only part of its scheduled duration.

$$\sum_{t=T_{start}(c)}^{T_{start}(c)+T_{opt}(c)-1} \sum_{i\in T} u_{so}(c,\ t,\ i) = T_{opt}(c)\left[\sum_{i\in T} u_{so}\left(c,\ T_{start}(c),\ i\right)\right],\ \ \forall c\in CT\ and\ T_{opt}(\tag{15}$$

$$\sum_{j=i}^{i+T_{opt}(c)-1} \sum_{t\in T} u_{si}(c,j,\ t) > T_{opt}(c)\left[\sum_{t\in T} u_{si}(c,i,\ t) - \sum_{t\in T} u_{si}(c,i-1,\ t)\right],\ \ \forall c\in CT,\ \forall \tag{16}$$

Constraint (16) imposes the continuity requirement on the incoming shifted load for the required duration $T_{opt}(c)$. For $i = 1$, the preceding incoming variable $u_{si}(c,i-1,t)$ is set to zero. Constraint (17) limits the total number of outgoing shifted intervals for each customer to the required number of operating intervals. Together, (15) – (17) are intended to preserve the

complete operating block and its continuity after rescheduling.

$$\sum_{t,\, i\in T} u_{so}(c,t,\ i) \le T_{opt}(c),\ \ \forall c\in CT. \tag{17}$$

For transferable loads, (18) ensures that total energy consumption remains unchanged after DR adjustment. The variables $P_{transfer-initial}(t)$ and $P_{transfer-final}(t)$ denote the initial and adjusted loads, respectively. Thus, energy consumption is redistributed across time intervals without changing its total over the scheduling horizon.

$$\sum_{t\in T} P_{transfer-final}(t)\Delta t = \sum_{t\in T} P_{transfer-initial}(t)\Delta t \tag{18}$$

Equation (19) calculates the adjusted transferable load by adding the upward adjustment $P_{DR-up}(t)$ and subtracting the downward adjustment $P_{DR-down}(t)$ from the initial load.

$$P_{transfer-final}(t) = P_{transfer-initial}(t) + P_{DR-up}(t) - P_{DR-down}(t),\ \forall t\in T. \tag{19}$$

Constraints (20) and (21) limit these adjustments according to the flexibility limit $\beta(t)$. The binary variable $u_{dr}(t)$ selects the adjustment direction, preventing simultaneous upward and downward adjustments within the same interval.

$$0\le P_{DR-up}(t) \le u_{dr}(t)\beta(t)P_{transfer-initial}(t), \forall t\in T. \tag{20}$$

$$0\le P_{DR-down}(t) \le \left(1 - u_{dr}(t)\right)\beta(t)P_{transfer-initial}(t), \forall t\in T. \tag{21}$$

The PV operating constraint in (22) limits generation at each time interval. The actual PV output $P_{PV}(t)$ must be non-negative and cannot exceed the available PV power $P_{PV-max}(t)$, as specified by the PV generation profile.

$$0\le P_{PV}(t) \le P_{PV-max}(t),\quad \forall t\in T. \tag{22}$$

The ESS operating constraints in (23) and (24) limit charging and discharging powers to the maximum power rating $P_{ESS-max}$. The binary variable $u_{ESS}(t)$ prevents simultaneous charging and discharging.

$$0\le P_{ESS-charge}(t) \le u_{ESS}(t)P_{ESS-max}\ , \forall t\in T. \tag{23}$$

$$0\le P_{ESS-discharge}(t) \le \left(1 - u_{ESS}(t)\right)P_{ESS-max}, \forall t\in T. \tag{24}$$

Equations (25) and (26) determine the stored energy at the end of each interval. Equation (25) uses the initial energy $E_{ESS-initial}$ for the first interval, whereas (26) uses the stored energy at the end of the preceding interval. Both equations account for charging and discharging power and the corresponding efficiency η_{ESS}.

$$E_{ESS}\left(t = t_1\right) = E_{ESS-initial} + \left(\eta_{ESS} P_{ESS-charge}(t) - \frac{P_{ESS-discharge}(t)}{\eta_{ESS}}\right)\Delta t, \quad \forall t \in T. \tag{25}$$

$$E_{ESS}\left(t > t_1\right) = E_{ESS}(t-1) + \left(\eta_{ESS} P_{ESS-charge}(t) - \frac{P_{ESS-discharge}(t)}{\eta_{ESS}}\right)\Delta t, \quad \forall t \in T. \tag{26}$$

Constraint (27) requires the stored energy at the end of the scheduling horizon to equal its initial value, establishing a cyclic energy condition. Constraint (28) maintains the stored energy between the lower limit $E_{ESS-min}$ and the upper limit $E_{ESS-max}$.

$$E_{ESS}\left(t = t_{24}\right) = E_{ESS-initial} \tag{27}$$

$$E_{ESS-min} \leq E_{ESS}(t) \leq E_{ESS-max}, \quad \forall t \in T. \tag{28}$$

The objective function in (1), together with the component definitions in (2)–(5) and constraints (6)–(28), forms the MILP model. The model is implemented in GAMS and solved using CPLEX, as illustrated in Figure 2.

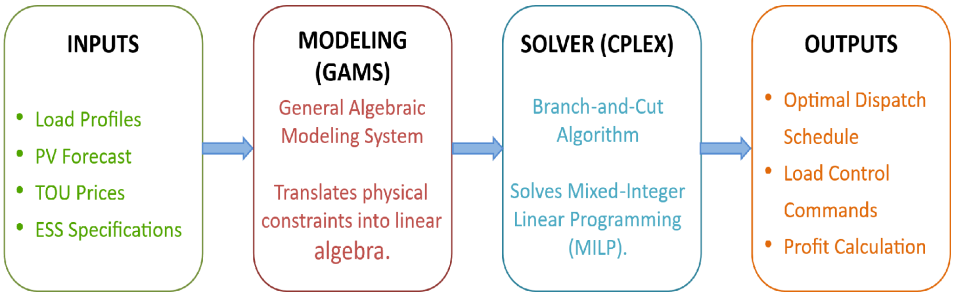


Figure 2. Flowchart of the proposed MILP scheduling methodology implemented in GAMS and solved by CPLEX.

RESULT AND DISCUSSION

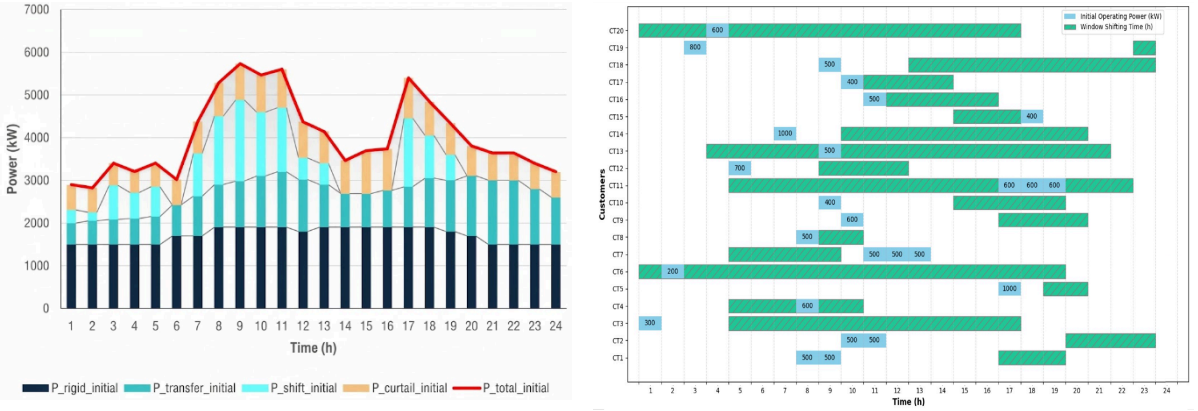
This section presents the case study and simulation results of the proposed LA scheduling model. Three operating scenarios are compared to evaluate the effects of PV, ESS, and DR integration on grid electricity purchases, load scheduling, and net operating profit.

A. Case Study

The optimal scheduling model developed in the previous section is applied to a test system. The model uses different load categories and energy resources as inputs and provides the optimized grid power purchase, load schedule, and operating cost as outputs. In the test system, the LA acts as an intermediary between the grid and end users, coordinating multiple load types and energy resources for cost-effective operation. Customer demand is divided into four categories: rigid, curtailable, shiftable, and transferable loads, as shown in Figure 3. These load profiles are synthetically generated but calibrated to reflect typical demand characteristics in Vietnam.

As shown in Figure 3, the rigid load represents the non adjustable baseline demand, ranging from 1500 kW during off-peak periods to 1900 kW during peak periods. The transferable load ranges from 500 kW to 1500 kW, with a maximum adjustment of 30% per hour. The curtailable load ranges from 500 kW to 1000 kW, and its maximum curtailment ratio is 30%. For shiftable loads, 20 customers are considered, representing commercial or industrial users with flexible operating schedules, such as production machinery, pumping systems, or

large HVAC units. These loads cannot be directly adjusted in power but can be shifted as a whole within their allowable operating windows. Their profiles and related constraints, including T_{start}, T_{opt}, T_{min}, T_{max}, and $P_{s-allow}$, are shown in Figure 3b.



(a) (b)

Figure 3. The LA's load profiles: (a) Initial profiles of each type of customers; (b) Initial operating power and allowable shifting time windows of shiftable customers.

On the supply side, the LA purchases electricity from the main grid under Vietnam's TOU tariff, with peak, regular, and off-peak prices of 3183, 1737, and 1084 VND/kWh, respectively [21]. It resells electricity to customers at a fixed rate of 1895 VND/kWh, as shown in Table 1, which is lower than many retail tariffs and therefore encourages customer participation.

Table 1. Electricity tariffs and assumed DR incentive rates

Type	Time period	Grid electricity tariff (VND/kWh) [21]	Customer tariff (VND/kWh)	Incentive rate (VND/kWh)		
				Curtailable	Transferable	Shiftable
Peak period	Hours 11-12, and hours 18-20	3,183	1,895	927.9	927.9	500
Regular period	Hours 5-10, hours 13-17, and hours 21-22	1,737	1,895	500.7	–	500
Off-peak period	Hour 1-4, and hours 23-24	1,084	1,895	325.2	162.6	500

To reduce grid dependency, the model includes a 2,500 kWp PV system and an ESS. The PV system supplies renewable energy during daytime hours, as shown in Figure 4. For simulation purposes, the PV operating cost is assumed to be 30 VND/kWh and is used as a simplified operating cost parameter. The ESS supports load management by storing energy and discharging it when needed. It has a maximum charge/discharge power of 500 kW, an energy capacity of 2000 kWh, an initial energy level of 600 kWh, and a charge/discharge efficiency of 95%, corresponding to a round trip efficiency of approximately 90%. The ESS operating cost is assumed to be 520 VND/kWh to represent battery cycling and maintenance effects in short term operation.

The LA also applies DR programs to improve operational flexibility. Customers receive incentive payments based on the DR type and adjustment period. Since official DR tariffs for customer-side loads are not yet available in Vietnam, the assumed incentive rates in Table 1 are included in the LA's operating costs. By coordinating grid purchases, PV generation, ESS operation, and DR incentives, the LA can better balance supply and demand while reducing operating costs.

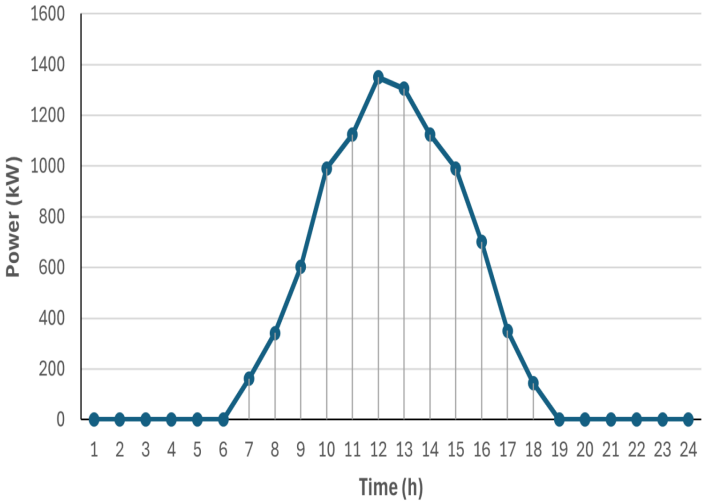


Figure 4. PV system's available power output.

B. Evaluation of the Roles of PV, ESS, and DR in LA Operation

Based on the load data presented earlier, the total customer demand is shown by the solid red line in Figure 3a. The daily peak reaches 5700 kW at hour 9, while the demand at hour 17 remains high at about 5400 kW. By contrast, the load drops to around 2820 kW from midnight to hour 2. This creates a peak to valley difference of nearly 2800 kW, which may put pressure on grid operation if the LA relies only on grid supply.

When PV is integrated into the LA, its output reaches the maximum value at hour 12, as shown in Figure 4. However, the load at this time is only about 78% of the daily peak. During the evening high-demand period, from hours 17 to 19, PV generation drops sharply. For example, PV output at hour 17 is only 351 kW, much lower than the load demand of 5400 kW. This mismatch indicates the need for additional flexibility from the ESS and DR programs.

To better understand the roles of PV, ESS, and DR, three scenarios are considered. In Scenario 1, the LA is supplied only by the main grid. In Scenario 2, the LA integrates PV and ESS, while in Scenario 3, the DR program is further added to the PV–ESS configuration. The grid power purchased by the LA in each scenario is presented in Figure 5.

Scenario 1: The LA is supplied only by the electricity grid

In Scenario 1, the LA relies entirely on electricity purchased from the main grid under the TOU tariff in Table 1. As shown in Figure 5, grid power demand reaches about 5700 kW during the high-demand periods, particularly hours 9–11 and hour 17. Since the LA has no internal RES, ESS, or DR support in this scenario, it achieves only a modest daily net profit of 0.276 million VND.

Scenario 2: The LA integrates PV and ESS

In Scenario 2, the LA integrates both PV and ESS systems. PV generation reduces grid purchases during daytime hours, especially from hours 6 to 18 when solar output is available. As shown in Figure 5, grid purchases during high-demand periods such as hours 10–11 decrease from about 5500 kW in Scenario 1 to around 4000–4500 kW in Scenario 2. At hour 12, when PV output reaches its daily peak, grid purchases fall to about 2500 kW, nearly 2000 kW lower than in the grid only case.

The ESS further supports the LA during the evening peak, when PV output is no longer

available. By charging during off-peak, low price, or surplus PV periods and discharging during high demand, high price hours, the ESS helps reduce grid dependency at critical times, as illustrated in Figure 6. As a result, integrating PV and ESS increases the LA's daily net profit from 0.276 million VND in Scenario 1 to 21.518 million VND in Scenario 2. This improvement is mainly due to lower daytime grid purchases from PV generation and energy shifting by the ESS under the TOU tariff.

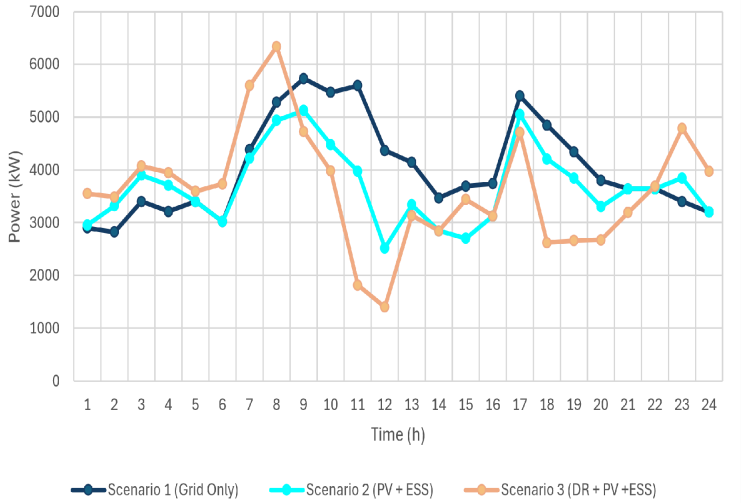


Figure 5. Comparison of the grid power purchased by the LA in three scenarios

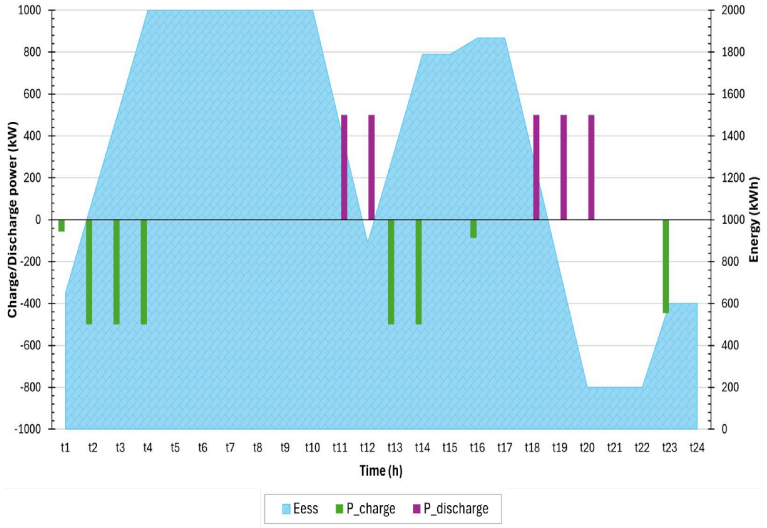


Figure 6. The ESS operating schedule in Scenario 2

Scenario 3: The LA integrates PV, ESS and DR program

Scenario 3 combines DR with PV and ESS and results in the lowest grid purchases among the three scenarios during several high price hours. At hour 12, grid purchases fall to approximately 1400 kW, corresponding to about 32% of Scenario 1 and 56% of Scenario 2 at that same hour. This percentage is an hour specific comparison and should not be interpreted as the average reduction over the entire peak tariff period. During the evening peak, when PV output is unavailable, grid demand remains approximately 2621 kW. Temporary increases at hour 8 and during off-peak periods indicate that the optimizer transfers part of the demand to lower price intervals.

Adding DR increases the LA's daily net profit from 21.518 million VND in Scenario 2 to 29.360 million VND in Scenario 3, even after accounting for customer incentive payments. This improvement mainly comes from load shifting, curtailment, and transferable load adjustments. Overall, the results show that DR works effectively with PV and ESS to reduce peak-hour grid dependence and improve LA's economic performance.

The detailed DR results further explain this improvement. For transferable loads, demand increases during off-peak periods, especially hours 1–4 and 23–24, and decreases during peak periods, including hours 11–12 and 18–20, as shown in Figure 7. The maximum reduction reaches about 450 kW, indicating that part of the demand is shifted from high-price to low-price periods. Curtailable loads, on the other hand, mainly support peak reduction. As shown in Figure 8, curtailment is mostly activated during peak-price periods, where reducing grid purchases brings the greatest economic benefit. During regular and off-peak periods, the curtailable load remains almost unchanged because curtailment is less cost-effective.

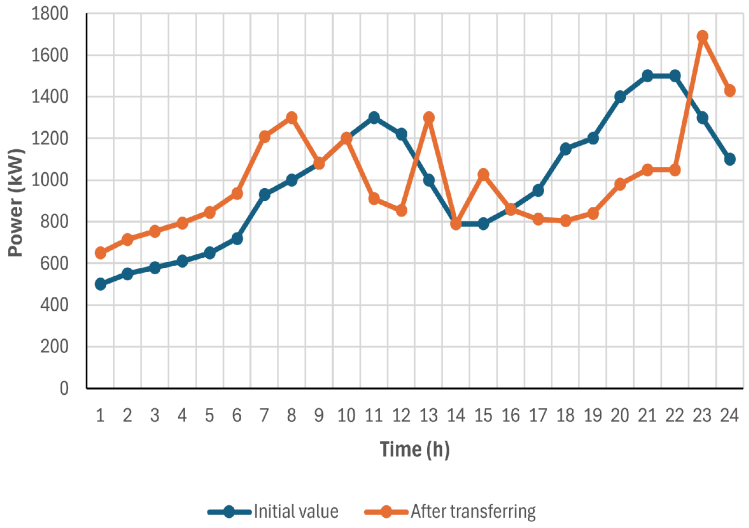


Figure 7. Transferable load profile before and after adjustment

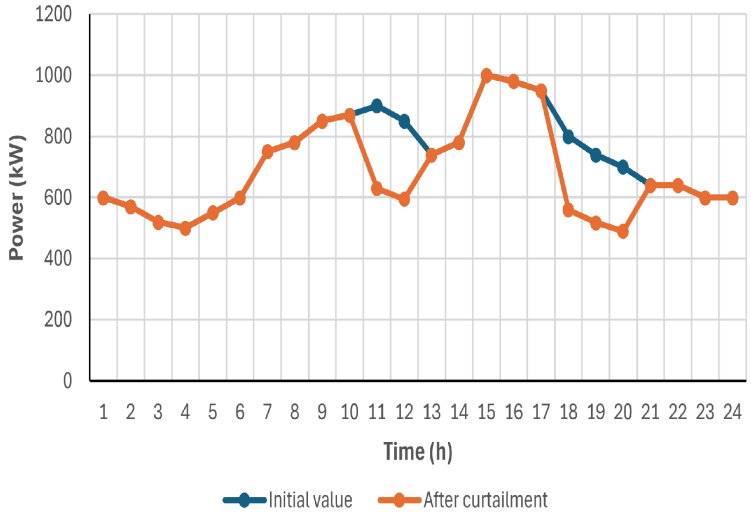


Figure 8. Curtailable load profile before and after curtailment.

For shiftable loads, Figure 3b shows that many customers originally operate during regular and peak periods. After optimization, most of them are rescheduled to lower price periods while still satisfying their operating constraints. As illustrated in Figure 9, CT2 is shifted from

hour 10 to hours 22–24, while CT11 is moved from hours 17–19 to hours 7–10. Loads already scheduled in off peak periods, or those whose allowable shifting windows fall in higher-price periods, generally remain unchanged. For example, CT1 keeps its schedule because its shifting window lies within the evening peak period, while CT19 remains unchanged because both its original schedule and allowable window are in off-peak periods.

The aggregated profile in Figure 10 confirms the effect of shiftable load scheduling. Before shifting, demand peaks around hours 8–10 and 17–18, reaching about 1900 kW. After optimization, part of the demand is moved to earlier or lower-price periods, and the demand during hours 10–12 and 18–19 is greatly reduced. Overall, the optimized schedule shifts demand away from the usual peak periods, helping reduce LA's peak demand and ease grid pressure.

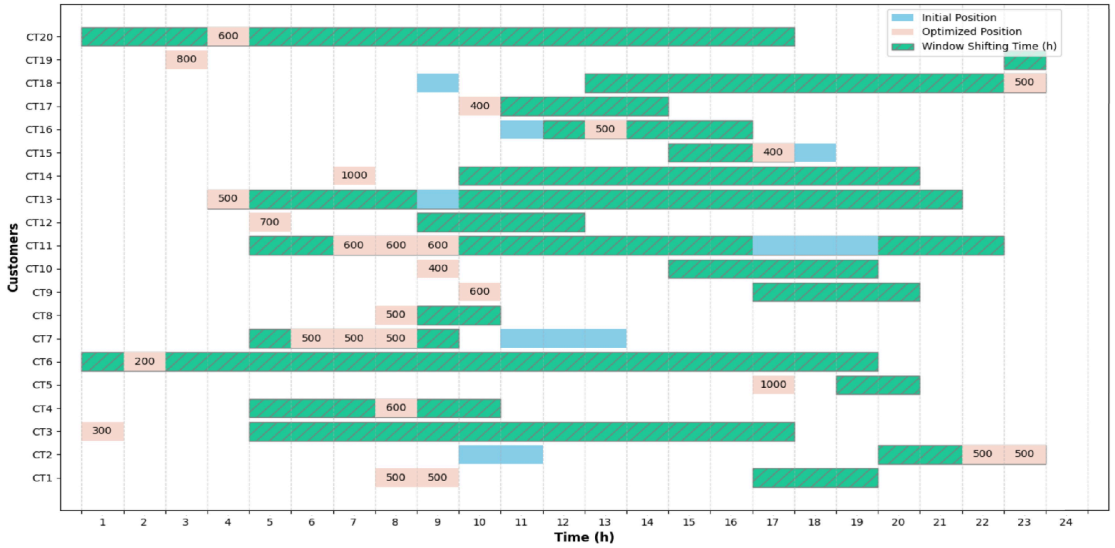


Figure 9. Shiftable load scheduling results showing the initial, optimized, and allowable shifting time windows for customers CT1–CT20

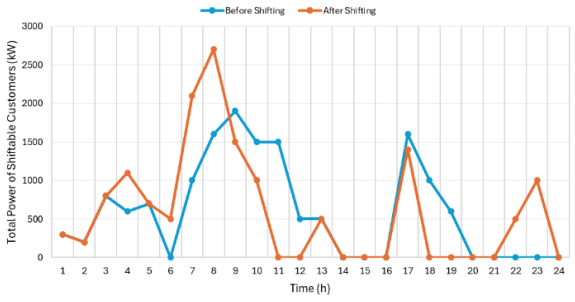


Figure 10. Aggregated load profile of shiftable customers before and after load shifting.

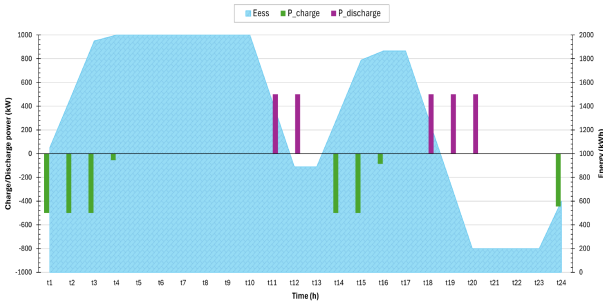


Figure 11. The ESS operating schedule in Scenario 3.

As shown in Figure 11, the ESS starts with an initial energy level of 600 kWh and charges during low price off-peak hours. Its energy reaches the maximum capacity of 2000 kWh by hour 4 and remains at this level until hour 10. The ESS discharges during hours 11–12, when electricity prices are highest, and charges again during hours 14–15 to prepare for the evening peak. From hours 18 to 20, its energy drops from above 1800 kWh to the minimum limit of 200 kWh as it supports peak demand. Overall, the ESS shifts energy from low-price to

high-price periods, reducing electricity purchasing costs and improving the LA's operating efficiency.

C. Limitations and Future Work

The reported results should be interpreted as deterministic, one-day operating results. The load profiles are synthetic, while demand and PV forecasts are treated as known; therefore, the case study does not establish out of sample performance under forecast error or customer uncertainty. In addition, the economic comparison excludes annualized PV and ESS investment costs, fixed operation and maintenance, battery degradation and replacement, financing assumptions, taxes, and project lifetime. The reported values consequently represent net operating profit under the stated short term assumptions rather than full investment profitability. The demand response incentive rates are also assumed because a complete customer-side compensation mechanism is not yet available for the studied context. Future work should evaluate measured or multiple day profiles, uncertainty-aware scheduling, sensitivity to incentive levels, and full life-cycle economics.

CONCLUSION

This study presents an operational optimization model for an LA that integrates distributed energy resources and multiple types of DR loads, including curtailable, transferable, and shiftable loads. The model maximizes the LA's net profit by coordinating internal PV and ESS resources with flexible load adjustments under Vietnam's TOU tariff, while also considering customer incentive payments. Under the stated short-term operating assumptions, the reported daily net operating profit increases from 0.276 million VND in the grid-only case to 21.518 million VND with PV and ESS and to 29.360 million VND when demand response is included. At hour 12 specifically, grid purchases in Scenario 3 are approximately 32% of those in Scenario 1. These results indicate that coordinated scheduling can reduce grid dependence during selected high price intervals and improve short-term operating performance. The main methodological contribution is the shiftable load formulation, which preserves both rated operating power and continuous operating duration after rescheduling. The findings remain conditional on the synthetic one-day profiles, deterministic forecasts, assumed incentive rates, and exclusion of capital and replacement costs. Before acceptance, the model should be supported by the requested validation or sensitivity analysis, solver-performance reporting, and a complete economic breakdown. Future work may extend the framework to measured data, uncertain PV and demand forecasts, rolling horizon operation, and investment feasibility assessment.

REFERENCES

[1] Vietnam News Agency, "Long-term strategies need to prepare for rising power demand," Vietnam Electricity, Jan. 2, 2025. Accessed: Oct. 7, 2025. [Online]. Available: https://en.evn.com.vn/d/en-US/news/Long-term-strategies-need-to-prepare-for-rising-power-demand-60-163-500430

[2] L. Li, X. Dou, H. Yang, Y. Fu, J. Yu, X. Huo, and C. Pang, "Dynamic aggregation method for load aggregators considering users' deviation of electricity," Electronics, vol. 13, no. 2, Jan. 2024, Art. no. 278, doi: 10.3390/electronics13020278.

[3] H. Yang, Z. Sun, X. Dou, L. Li, J. Yu, X. Huo, and C. Pang, "Optimal scheduling and compensation pricing method for load aggregators based on limited peak shaving budget and time segment value," Energies, vol. 17, no. 22, Nov. 2024, Art. no. 5759, doi: 10.3390/en17225759.

[4] C. Zhang, Z. Du, P. Wu, Q. Sun, Y. Li, and Y. Zhang, "Flexible load scheduling methods for load aggregators," J. Phys.: Conf. Ser., vol. 1920, no. 1, May 2021, Art. no. 012024, doi: 10.1088/1742-6596/1920/1/012024.

[5] A. Pinyo and A. Bangviwat, “Smart contracts-based demand response bidding mechanism to enhance the load aggregator model in Thailand,” Energies, vol. 16, no. 8, Apr. 2023, Art. no. 3606, doi: 10.3390/en16083606.
[6] M. Yu, W. Sun, Y. Zhao, X. Wang, J. Du, X. Qian, and J. Sun, “Optimal scheduling model of load aggregator on demand side under demand response,” Eng. Rep., vol. 7, no. 3, Mar. 2025, Art. no. e70017, doi: 10.1002/eng2.70017.
[7] Y. Zhang, J. Yang, J. Li, Y. Han, Z. Zhao, X. Du, M. Liu, and D. Liu, “The research on systems of charging load aggregators participating in market transactions based on Internet of Vehicles,” IOP Conf. Ser.: Earth Environ. Sci., vol. 791, no. 1, Jun. 2021, Art. no. 012138, doi: 10.1088/1755-1315/791/1/012138.
[8] G. Xu, S. Song, Y. Li, Y. Lu, Y. Zhao, L. Zhang, F. Wang, and Z. Song, “Application of deep reinforcement learning in electricity demand response market: Demand response decision-making of load aggregator,” MethodsX, vol. 12, Jun. 2024, Art. no. 102735, doi: 10.1016/j.mex.2024.102735.
[9] X. Wang, Y. Su, W. Xu, S. Zhang, and Y. Zhang, “A market decision-making model for load aggregators with flexible load,” Front. Energy Res., vol. 10, Jan. 2023, Art. no. 1030076, doi: 10.3389/fenrg.2022.1030076.
[10] B. Jangid, P. Mathuria, and V. Gupta, “A flexible load aggregation framework for optimal distribution system operation,” Sustain. Energy Grids Netw., vol. 35, Sep. 2023, Art. no. 101117, doi: 10.1016/j.segan.2023.101117.
[11] H. Zhang, Y. Tian, Y. Zhao, Q. Liu, and N. Zhang, “Economic dispatch of generation load aggregators based on two-stage robust optimization,” Front. Energy Res., vol. 11, Aug. 2023, Art. no. 1258689, doi: 10.3389/fenrg.2023.1258689.
[12] J. Lu, Z. Xie, H. Xu, and J. Liu, “Optimizing joint bidding and incentivizing strategy for price-maker load aggregators based on multi-task multi-agent deep reinforcement learning,” IEEE Access, vol. 12, pp. 163988–164001, 2024, doi: 10.1109/ACCESS.2024.3491189.
[13] C. Xie, R. Zhu, X. Xu, and Y. Sun, “Optimization strategy for demand response participation of heterogeneous flexible load aggregators based on inner approximation method,” Int. Trans. Electr. Energy Syst., vol. 2025, no. 1, 2025, Art. no. 5460409, doi: 10.1155/etep/5460409.
[14] L. Zheng, J. Zheng, H. Tang, Z. Liu, T. Li, J. Lu, and Z. Hu, “Multi-objective optimal scheduling of distribution networks with load aggregator involvement,” Energy Rep., vol. 14, pp. 486–499, Dec. 2025, doi: 10.1016/j.egyr.2025.06.010.
[15] H. Yang, Z. Zhang, R. Liang, and W. Zhao, “Research on time-of-use compensation pricing strategies for load aggregators based on user demand response,” Front. Energy Res., vol. 12, Sep. 2024, Art. no. 1442194, doi: 10.3389/fenrg.2024.1442194.
[16] H. S. Ryu, H. J. Kim, and M. K. Kim, “Two-level optimal bidding strategy for load aggregator based on a data-driven approach combined with LSTM-based forecasting and agent-based models,” IEEE Access, vol. 11, pp. 89249–89264, 2023, doi: 10.1109/ACCESS.2023.3306409.
[17] Y. Zhang, B. Zou, Y. Liang, Y. Luo, M. Chen, J. Ye, S. Li, Y. Li, X. Hu, and W. Pan, “Potential assessment of coordinated regulation of power load of emerging industrial users based on extreme scenarios of electric vehicle aggregators,” IET Renew. Power Gener., vol. 18, no. 16, pp. 4004–4019, Dec. 2024, doi: 10.1049/rpg2.13120.
[18] B. Jangid, P. Mathuria, and V. Gupta, “A hierarchical scheduling framework for DSO and shiftable load aggregator,” Electr. Power Syst. Res., vol. 225, Dec. 2023, Art. no. 109861, doi: 10.1016/j.epsr.2023.109861.
[19] M. R. Bussieck and A. Meeraus, “General Algebraic Modeling System (GAMS),” in Modeling Languages in Mathematical Optimization, J. Kallrath, Ed. Boston, MA, USA: Springer, 2004, ch. 8, pp. 137–157, doi: 10.1007/978-1-4613-0215-5_8.
[20] IBM, “ILOG CPLEX Optimization Studio.” Accessed: Mar. 31, 2022. [Online]. Available: https://www.ibm.com/products/ilog-cplex-optimization-studio

[21] Vietnam Electricity, “Retail electricity tariff (Decision No. 1279/QD-BCT dated 9 May 2025 of Ministry of Industry and Trade),” May 9, 2025. Accessed: Oct. 8, 2025. [Online]. Available: https://en.evn.com.vn/d/en-US/news/RETAIL-ELECTRICITY-TARIFF-Decision-No-1279QD-BCT-dated-9-May-2025-of-Ministry-of-Industry-and-Trade-60-28-252

BIOGRAPHIES OF AUTHORS



Nhung Nguyen-Hong received the B.S. and M.Sc. degrees in electrical engineering from the Department of Electric Power Systems, Hanoi University of Science and Technology, Hanoi, Vietnam, in 2008 and 2010, respectively. She is currently working toward the Ph.D. degree with the Graduate School of Energy and Environment, Waseda University, Tokyo, Japan. Her research interests include power system optimization and integration of renewable energy sources in the power systems.



Khang Trieu-Phuc was born in Thanh Hoa, Vietnam in 2003. He received the B.S. degree in Electrical engineering and renewable energy from Hanoi University of Science and Technology (HUST) in 2025. He is presently pursuing the M.S. degree in electrical engineering, focusing on power systems. Since 2026, he has been working as an electrical engineer at the High-Voltage Grid Enterprise, Thanh Hoa Power Company.



Quan Tran-Duc was born in Nghe An, Vietnam in 2003. He received the B.S. degree in electrical engineering and renewable energy from Hanoi University of Science and Technology (HUST) in 2025. Since 2026, he has been working as a Fuel and Electrical Auxiliary Operator at the Quang Trach 1 Thermal Power Plant.